Journal of Computational Applied Mechanics 2022, 53(4): 494-509

DOI: 10.22059/JCAMECH.2022.348047.749

RESEARCH PAPER

Radiation effect on the flow of Magneto Hydrodynamic nanofluids over a stretching surface with Chemical reaction

Gobburu Sreedhar Sarma [a*], Ganji Narender [a], Kamatam Govardhan [b]

[a] *Department of Humanities & Sciences (Mathematics), CVR College of Engineering, Jawaharlal Nehru Technological University, Hyderabad, Telangana State, India*

[b] *Department of Mathematics, GITAM University, Hyderabad, Telangana State, India*

Abstract

The flow of nanofluids over a stretching surface has gotten a lot of attention because of its many uses in industry and engineering. In recent years, heat and mass transfer in magneto hydrodynamic nanofluids has become a focus of research. The steady two-dimensional Magneto hydrodynamic nanofluid flow across a stretched sheet is examined in this study under the effect of radiation and chemical reaction. The similarity transformations which are used to convert the partial differential equations into ordinary differential equations, these equations are solved by Mathematica12.0. On a visual level, the impacts of different dimensionless parameters on non-dimensional velocity, temperature and concentration profiles have been investigated. It is observed that, the thermal radiation enhances the temperature profiles and chemical reaction diminishes the concentration. The parameters of physical interest i.e., Nusselt number decreases and Sherwood number increases with the increasing of the effect of radiation and chemical reaction. In several exceptional circumstances, the resulting numerical findings are compared to previously published results and excellent agreement is found.

Keywords: Nano fluids; Stretching sheet; Magnetic field; Radiation; Chemical reaction.

1. Nomenclature

x, y	Cartesian coordinates
u, v	Horizontal and vertical velocity components
$u_w(x)$	Stretching velocity
μ_f	Dynamic viscosity of base fluid
ν	Kinematic viscosity
k_f	Thermal conductivity
a	Stretching rate
ρ_f	Density
P	Fluid pressure

[*] Corresponding author. Tel.: +91 9441007425

E-mail address: sarma.sreedhar@gmail.com

σ^*	Fluid Electric conductivity
B_0	Applied magnetic field intensity
α	Thermal diffusivity
τ	*Heat* capacity ratio for fluid and nanoparticles
D_B	Brownian diffusion
T	Local temperature of the fluid
C	Concentration distributions
$(\rho c)_f$	Fluid's productive heat capacity
s	Suction or injection parameter
T_w	Temperature of the sheet
T_∞	Temperature of the fluid far away from the sheet
D_T	Thermophoresis diffusion coefficient
C_w	Solid volume friction of the sheet
Sh_r	Reduced Sherwood number
G	Gravitational acceleration
B	Volumetric expansion coefficient of the fluid
ϕ_w	Nanoparticle volume fraction at the surface
ϕ_∞	Ambient nanoparticle volume fraction attained as y tends to be infinite
Ra_x	Local Rayleigh number
C_∞	Solid volume friction far away from the sheet
E_c	Eckert number
ϕ	Dimensionless concentration
f	Dimensionless stream function
θ	Dimensionless temperature
ψ	Stream function
P_r	Prandtl number
C_f	Local skin friction coefficient
η	Dimensionless space variable
$(\rho c)_p$	Nanoparticles' productive heat capacity
Le	Lewis number
N_b	Browian motion parameter
N_t	Thermophoresis parameter
M	Magnetic Parameter
Re_x	Reynolds number
K_c	Chemical reaction parameter
R	Radiation Parameter
Nu_r	Reduced Nusselt number

2. Introduction

Nanofluids, which are liquids with nano-sized particles suspended (usually less than 100 nm), are considered promising for heat transfer fluid design. The primary goal of nanofluids is to achieve the best possible thermal properties at the lowest possible concentrations by ensuring uniform dispersion and stable suspension of nanoparticles in host fluids. A colloidal solvent with scattered nanometer-sized particles (1-100 nm) is referred to as a nanofluid. High-tech industries like microelectronics, transportation, manufacturing, and metallurgy are experiencing one of the most pressing technical challenges: cooling. Nanofluids can significantly improve the thermal characteristics of host fluids when utilized as coolants.

Nanofluids are most commonly used in the thermal management of industrial and consumer products, where effective cooling is needed to achieve functions and ensure long-term reliability. Nanofluids have a wide range of tribological and medical applications. Nanofluids have been shown in recent studies to increase the performance of real-world devices and systems like automatic transmissions. More research work is going on with the nanofluids through a stretching sheet. The heat transfer of nanofluids through a linearly stretched sheet with the impact of a magnetic field was discussed by S. Mansur et al. [1] and MAA. Hamad [2]. The effect of viscous dissipation on these Nanofluids was studied by the following researchers. Heat and mass transfer in MHD nanofluid over a stretching surface with viscous dissipation was examined by K. Govardhan et al. [3]. The numerical solution of MHD nanofluid over a stretching surface with chemical reaction and viscous dissipation was also studied by G. Narender et al. [4].

The role of thermal radiation in heat transfer analysis is crucial in the design of many advanced energy conversion systems that operate at higher temperatures. Radiation is frequently emitted by hot walls and the working fluid within these systems. The effect of radiation on Maxwell nanofluid was analyzed by Narender et al. [4] and heat transfer of unsteady Hybrid nanofluid flow was discussed by Sreedevi et al. [5]. MA. Seddeek and MS. Abdelmeguid [6] examined the effects of radiation and thermal diffusivity on heat transfer over a stretching surface with variable heat flux.

In recent years, the importance of coupled heat and mass transport with chemical reactions in various processes has sparked an interest. Evaporation at the water's surface, energy transfer in a wet cooling tower, movement in a desert cooler, and drying are all examples of simultaneous heat and mass transfer. More research articles were published on nanofluids over a stretching surface with the impact of chemical reactions. The study of bioconvective nanofluid flow with buoyancy effect and the chemical reaction was done by A. Shafiq et al. [7]. G. Narender et al. [8] explored radiative magnetohydrodynamics viscous nanofluid due to convective stretching sheet with the chemical reaction. The magnetohydrodynamic peristaltic flow of a nanofluid in a restricted artery was investigated for various types of nanoparticles by Devaki et al. [9]. There are many other related articles in similar fields that can be considered [10-51].

The focus of this article is to extend the work of [52]. In this article, magnetohydrodynamic nanofluids through a stretching sheet under the influence of chemical reactions and radiation are analyzed. Graphs are used to illustrate the impact of various non-dimensional parameters on temperature, concentration, and velocity profiles.

3. Mathematical Analysis

According to Ref. [53], a uniform magnetic field B_0 is applied along *the y*-direction (see Figure 1). The governing equations are:

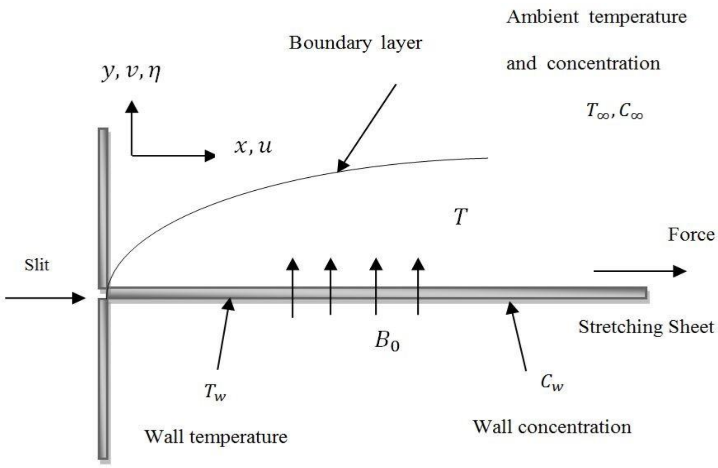

Fig 1: Physical model

$$\frac{\partial u}{\partial x}+\frac{\partial v}{\partial y}=0 \tag{1}$$

$$u\frac{\partial u}{\partial x}+v\frac{\partial u}{\partial y}=-\frac{1}{\rho_f}\frac{\partial p}{\partial x}+\nu\left(\frac{\partial^2 u}{\partial x^2}+\frac{\partial^2 u}{\partial y^2}\right)-\frac{\sigma^* B_0^{\,2}}{\rho_f}u, \tag{2}$$

$$u\frac{\partial v}{\partial x}+v\frac{\partial v}{\partial y}=-\frac{1}{\rho_f}\frac{\partial p}{\partial y}+\nu\left(\frac{\partial^2 v}{\partial x^2}+\frac{\partial^2 v}{\partial y^2}\right), \tag{3}$$

$$u\frac{\partial T}{\partial x}+v\frac{\partial T}{\partial y}=\alpha\left(\frac{\partial^2 T}{\partial x^2}+\frac{\partial^2 T}{\partial y^2}\right)+\tau\left\{D_B\left(\frac{\partial C}{\partial x}\frac{\partial T}{\partial x}+\frac{\partial C}{\partial y}\frac{\partial T}{\partial y}\right)+\left(\frac{D_T}{T_\infty}\right)\left[\left(\frac{\partial T}{\partial x}\right)^2+\left(\frac{\partial T}{\partial y}\right)^2\right]\right\}$$
$$+\frac{\mu_f}{(\rho c_p)_f}\left(\frac{\partial u}{\partial y}\right)^2+\frac{\sigma^* B_0^{\,2}}{(\rho c_p)_f}u^2-\frac{1}{\rho c_p}\frac{\partial q_r}{\partial y} \tag{4}$$

$$u\frac{\partial C}{\partial x}+v\frac{\partial C}{\partial y}=D_B\left(\frac{\partial^2 C}{\partial x^2}+\frac{\partial^2 C}{\partial y^2}\right)+\left(\frac{D_T}{T_\infty}\right)\left(\frac{\partial^2 T}{\partial x^2}+\frac{\partial^2 T}{\partial y^2}\right)-K_1(C-C_\infty) \tag{5}$$

The BCs are given as:

$$u=u_w(x)=ax,\ v=s,\ T=T_w,\ C=C_w \quad \text{when} \quad y=0,$$
$$u=0,\ v=0,\ C=C_\infty,\ T=T_\infty, \quad \text{when} \quad y\to\infty \tag{6}$$

To illustrate the radiative heat flux, the Roseland approximation is utilised.

$$q_r=-\frac{4\sigma^*}{3\delta}\frac{\partial T^4}{\partial y}, \tag{7}$$

Taylor's series is used to expand T^4 about T_∞. Omitting the higher-order terms in the Taylor's series and assume that temperature differences in the fluid are very small. The below approximation is

$$T^4\cong T_\infty^{\,3}T-3T_\infty^{\,4} \tag{8}$$

Using Eq. (7) and Eq. (8) in equation Eq. (4)
we get

$$\frac{\partial q_r}{\partial y}=-\frac{16\sigma^*}{3\delta}\frac{\partial^2 T^4}{\partial y^2} \tag{9}$$

The following dimensionless quantities are now introduced.

$$f(\eta)=\frac{\psi}{\alpha Ra_x^{1/4}},\quad \theta(\eta)=\left(\frac{T-T_\infty}{T_w-T_\infty}\right),\quad \phi(\eta)=\left(\frac{C-C_\infty}{C_w-C_\infty}\right) \tag{10}$$

Where ψ is a stream function satisfying $u=\dfrac{\partial\psi}{\partial y},\quad v=-\dfrac{\partial\psi}{\partial x}$ (11)

The governing boundary layer equations Eq. (1) – Eq. (5) corresponding to the boundary conditions Eq. (6) transformed into the below nonlinear O.D.Es using similarity solution in Ref. [52].

$$f'''+\left(\frac{1}{4P_r}\right)\left[3ff''-2(f')^2\right]-Mf'=0 \tag{12}$$

$$\left(1+\frac{4}{3}R\right)\theta''+\frac{3}{4}f\theta'+N_b\phi'\theta'+N_t(\theta')^2+E_c(f'')^2+M\ E_c\ (f')^2=0 \tag{13}$$

$$\phi''+\frac{3}{4}Le\ f\ \phi'+\left(\frac{N_t}{N_b}\right)\theta''-K_c\ Le\ \phi=0 \tag{14}$$

The boundary conditions are as follows:

$$f(0)=s,\ f'(0)=1,\ \theta(0)=1,\ \phi(0)=1,$$
$$f'(\infty)=0,\ \ \theta(\infty)=0,\ \ \phi(\infty)=0 \tag{15}$$

The dimensionless parameters are described by:

$$\eta=\frac{y}{x}Ra_x^{1/4},\ P_r=\left(\frac{\nu}{\alpha}\right),\ Le=\left(\frac{\alpha}{D_B}\right),\ N_b=\frac{(\rho c)_p(\phi_w-\phi_\infty)}{(\rho c)_f\,\alpha},\ N_t=\frac{(\rho c)_p D_T(T_w-T_\infty)}{(\rho c)_f\,\alpha T_\infty}$$

$$M=\frac{\sigma^* B_0^{\ 2}}{\mu_f}L^2,\ L=\sqrt[3]{\frac{\nu\alpha Ra_x^{1/4}}{(1-\phi_\infty)\beta g(T_w-T_\infty)}},\ E_c=\frac{\sqrt[3]{[(1-\phi_\infty)\beta g]^2\left[\dfrac{\nu\alpha Ra_x}{(T_w-T_\infty)}\right]}}{(C_p)_f},$$

$$Ra_x=\frac{(1-\phi_\infty)\beta g(T_w-T_\infty)x^3}{\nu\alpha},\ R=\frac{4\sigma^* T_\infty^{\ 3}}{k^* k},\ K_c=\left(\frac{K_1}{a}\right)$$

The surface drag coefficient C_f , the reduced Nusselt number Nu_r and the Mass transfer rate Sh_r [52] are given as:

$$f''(0)=\frac{1}{2}\left(\frac{P_r\,\mathrm{Re}_x^{\ 2}}{Ra_x^{\frac{3}{4}}}\right)C_f,\quad Nu_r=-\theta'(0),\quad Sh_r=-\phi'(0)$$

4. Numerical Results and Discussion

The nonlinear and non-dimensional system of equations (12) – (14) along with boundary conditions (15) were numerically solved in symbolic computational software Mathematica 12.0 using the NDsolve algorithm. Mathematica carried out numerical solutions of nonlinear differential equations for which no exact solution can be written. The solution is given in terms of an interpolating function, which is a table of values of the unknown function for different values of independent variable. A unique feature of NDsolve is that given PDEs and the solution domain is symbolic form, ND solve automatically chooses numerical methods that appear best suited to the problem structure. The impact of the non-dimensional parameters Brownian motion parameter $\left(N_b\right)$, Magnetic Parameter $\left(M\right)$, Prandtl number(P_r), Radiation parameter $\left(R\right)$, Lewis number $\left(Le\right)$, Thermophoresis parameter $\left(N_t\right)$, Chemical reaction parameter $\left(K_c\right)$, Eckert number $\left(E_c\right)$ on different profiles have been discussed through graphs.

4.1 *Validation of Results*

The results for Nu_r and Sh_r are compared with the results of Nader Y. Abd Elazem [52] for different values of $P_r=1,\ \ s=0.01,\ M=1,\ Le=1, E_c=0.01 R=0$ and $K_c=0$ without the influence of chemical reaction and radiation in Table 1. The comparison reveals that for each value of N_b and N_t, there is good agreement. The computations of Nu_r and Sh_r are determined in Table 2 for various values of R and K_c. We can observe that, the Nusselt number diminishes whereas the Sherwood number increases with the rise of R and K_c

Table 1- Variation of $Nu_r = -\theta'(0)$ and $Sh_r = -\phi'(0)$ for N_t and N_b when $P_r = 1,\ s = 0.01,\ M = 1,\ Le = 1, E_c = 0.01\, R = 0$ and $K_c = 0$

N_t	N_b	Nu_r		Sh_r	
		Nader Y. Abd Elazem [52]	Present Result	Nader Y. Abd Elazem [52]	Present Result
0.1	0.1	0.18658	0.1854023	0.322289	0.3236993
0.1	0.3	0.150689	0.1501344	0.403315	0.4085107
0.1	0.5	0.11767	0.1163234	0.418986	0.4191217
0.3	0.1	0.166257	0.1662198	0.159911	0.1598863
0.3	0.3	0.132122	0.1327950	0.367966	0.3643826
0.3	0.5	0.100782	0.1001809	0.408024	0.4065191
0.5	0.1	0.147136	0.1434736	0.0592868	0.052202
0.5	0.3	0.11468	0.1151582	0.351229	0.352741
0.5	0.5	0.0849405	0.0843851	0.407115	0.390217

Table 2- Impact of Nu_r and Sh_r with R and K_c when

$$P_r = 1, N_b = N_t = 0.1, Le = 1, s = 0.01, M = 1, E_c = 0.01$$

R	$K_c = 0$		$K_c = 0\cdot 2$		$K_c = 0\cdot 4$		$K_c = 0\cdot 6$		$K_c = 0\cdot 8$	
	Nu_r	Sh_r	Nu_r	Sh_r	Nu_r	Sh_r	Nu_r	Sh_r	Nu_r	Sh_r
0	0.390222	0.157817	0.383609	0.477282	0.380559	0.673147	0.378681	0.82276	0.377362	0.947537
0.2	0.333715	0.209691	0.329533	0.514255	0.327637	0.702238	0.326482	0.846691	0.325679	0.967746
0.4	0.295673	0.245906	0.292812	0.538856	0.291527	0.721149	0.290751	0.862034	0.290213	0.980585
0.6	0.268654	0.272444	0.266575	0.556186	0.265648	0.734211	0.265089	0.872505	0.264704	0.989279
0.8	0.248639	0.292625	0.247058	0.568946	0.246354	0.74367	0.245932	0.880011	0.245641	0.995467

The impact of R on temperature profile and concentration profile are presented respectively in Figure 2 and Figure 3. The temperature distribution appears to grow as R increases, whereas the nanoparticle concentration falls as R increases. Radiation has the effect of accelerating heat transmission; thus it should be kept to a minimum to aid in the cooling process.

Figure 4 show that, the concentration profile rapidly declines as the chemical reaction K_c is increased. i.e., as K_c grows, the number of solute molecules performing chemical reactions increases, tend to decrease in the concentration field. Hence the concentration boundary layer thickness is reduced.

The effect of Magnetic parameter (M) on dimensionless velocity and temperature profiles is plotted in Figure 5 and Figure 6. As M is increased, the velocity profiles decrease from Figure 5. Since the impact of magnetic field creates a Lorentz force that resists the motion of the fluid. So, the velocity of the fluid is decreased. From Figure 6, we can observe that the profile of temperature rises as the magnetic parameter is increased.

Figure 7 displays the Prandtl number influence on $\theta(\eta)$. When the Prandtl number increases, a decrease in the thermal conductivity takes place which ultimately guides to a reduction in the temperature field $\theta(\eta)$. An increment in the Prandtl number is an indication that the convective transport is dominant to the diffusive transport in the nanofluid.

Figure 8 is utilized to represent the influence of Le on $\phi(\eta)$. It is analyzed that an increment in the Lewis number the concentration boundary layer's thickness decreases. Lewis number is the ratio of thermal diffusivity to mass diffusivity.

Figure 9 shows the effect of E_c on dimensionless temperature profile. Eckert number E_c is the relationship between the kinetic energy of fluid particles and the enthalpy of the boundary layer. The kinetic energy of the fluid particles is boosted by higher values E_c. As a result, the temperature of the fluid increases slightly, which increases the thickness of the thermal boundary layer.

Figures 10 and 11 shows the effect of the N_b on $\theta(\eta)$ and $\phi(\eta)$. It is observed that rise in the values of N_b, the temperature profile marginally rises. This is due to the fact that as N_b grows, the mobility of the nanoparticles rises substantially, which increases the kinetic energy. As a result, the temperature rises and the thickness of the thermal boundary layer grows. As N_b rises, the concentration of the fluid as well as the thickness of the concentration boundary layer diminish.

Figure 12 and Figure 13 demonstrate the influence of the N_t on $\theta(\eta)$ and $\phi(\eta)$. When the impacts of thermophoretic increases, nanoparticles move from the heated area of the surface to the cold ambient fluid, raising the temperature at the boundary. This will result in a thickening of the thermal boundary layer. The thickness of nanoparticle concentration increases for N_t.

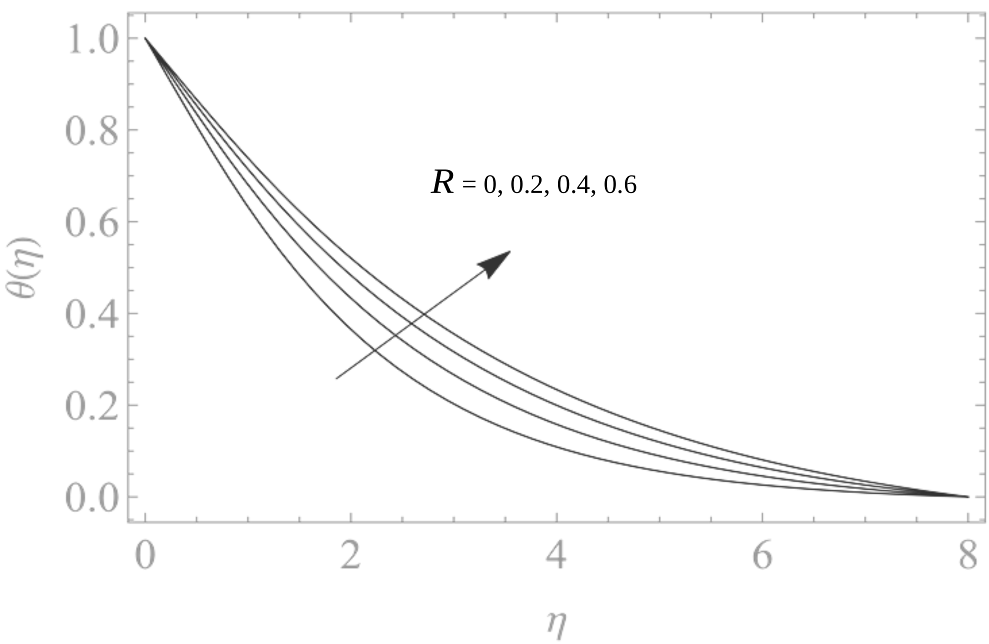

Fig 2: Impact of R on $\theta(\eta)$ with

$P_r = 1,\ Le = 1,\ s = 0.01,\ ,E_c = 0.01, M = 1, K_c = 0.5, N_b = 0.1, N_t = 0.1, \inf = 8$

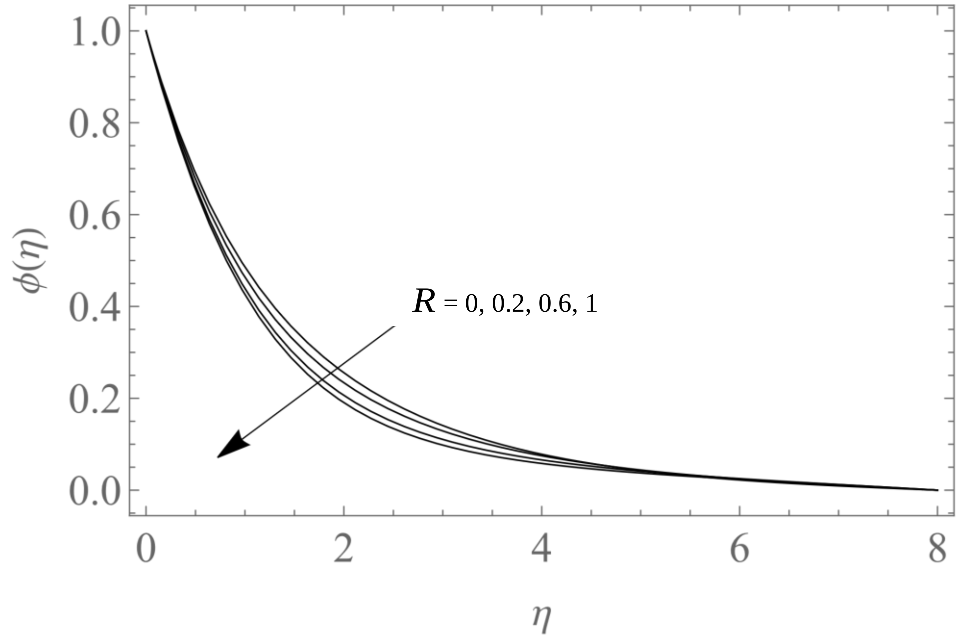

Fig 3: Impact of R on $\phi(\eta)$ with

$P_r = 1,\ Le = 1,\ M = 1,\ E_c = 0.01,\ s = 0.01,\ K_c = 0.5,\ N_b = 0.1,\ N_t = 0.1, \inf = 8$

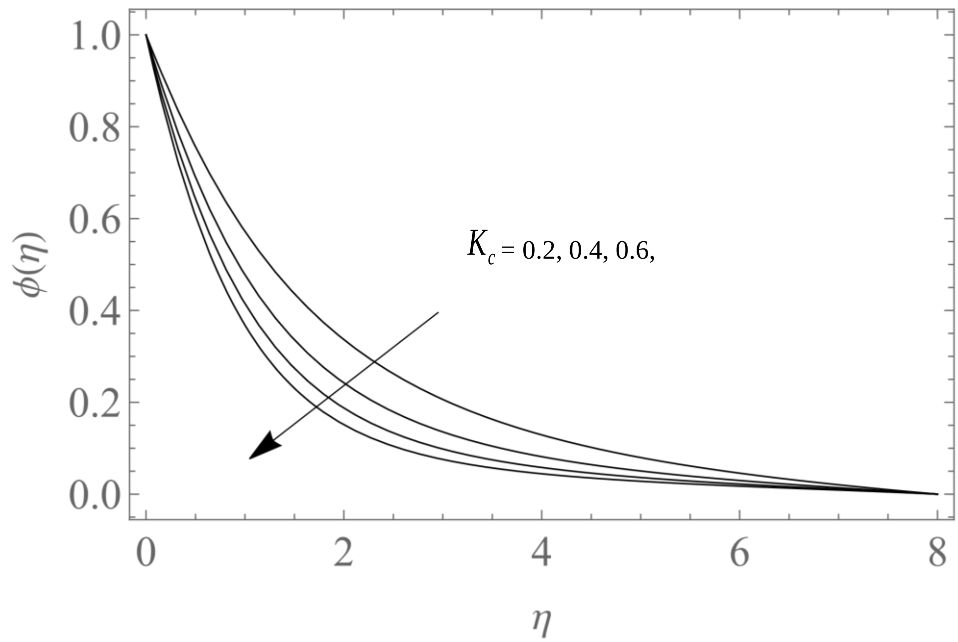

Fig 4: Impact of K_c on $\phi(\eta)$ with

$P_r = 1,\ Le = 1,\ M = 1,\ E_c = 0.01,\ s = 0.01,\ K_c = 0.5, \inf = 8,\ N_b = 0.1,\ N_t = 0.1,\ R = 0.5$

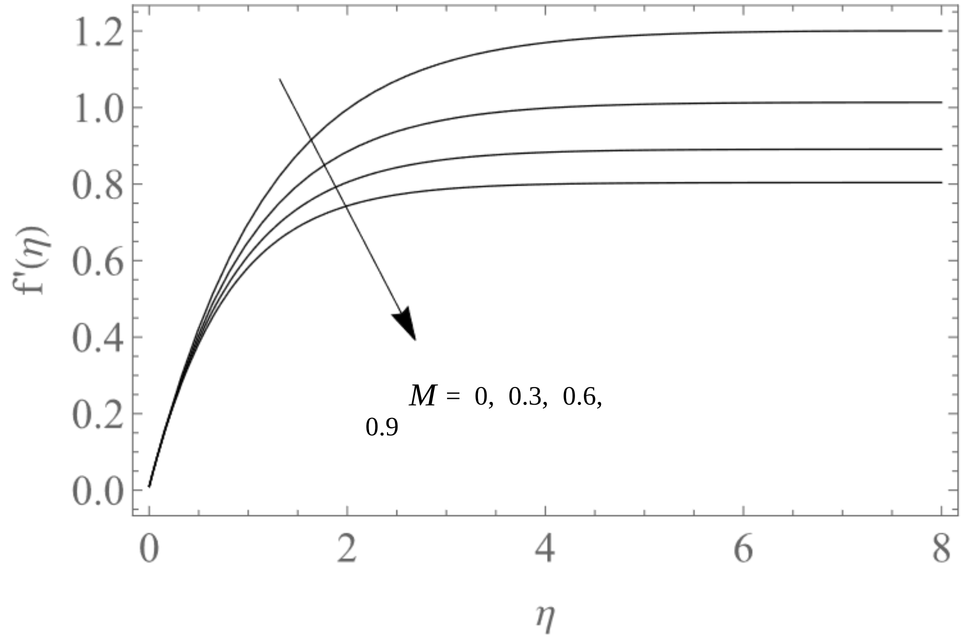

Fig 5: Impact of M on velocity profile with
$P_r = 1,\ Le = 1,\ E_c = 0.01, K_c = 0.5, \inf = 8, s = 0.01, R = 0.5, N_b = 0.1, N_t = 0.1$

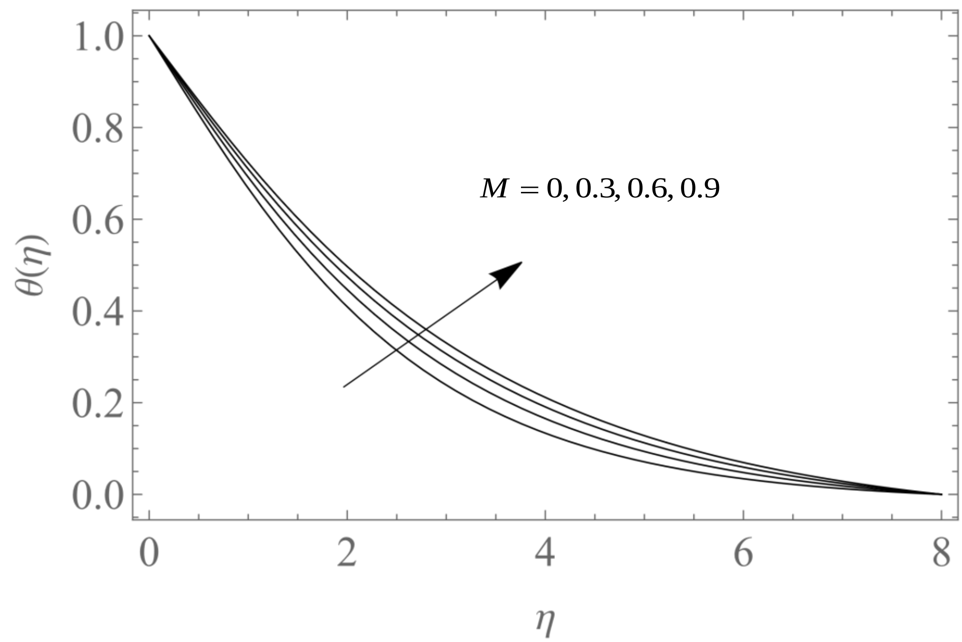

Fig 6: Impact of M on $\theta(\eta)$ with
$P_r = 1,\ Le = 1, M = 1, E_c = 0.01, K_c = 0.5, s = 0.01, \inf = 8, R = 0.5, N_b = 0.1, N_t = 0.1$

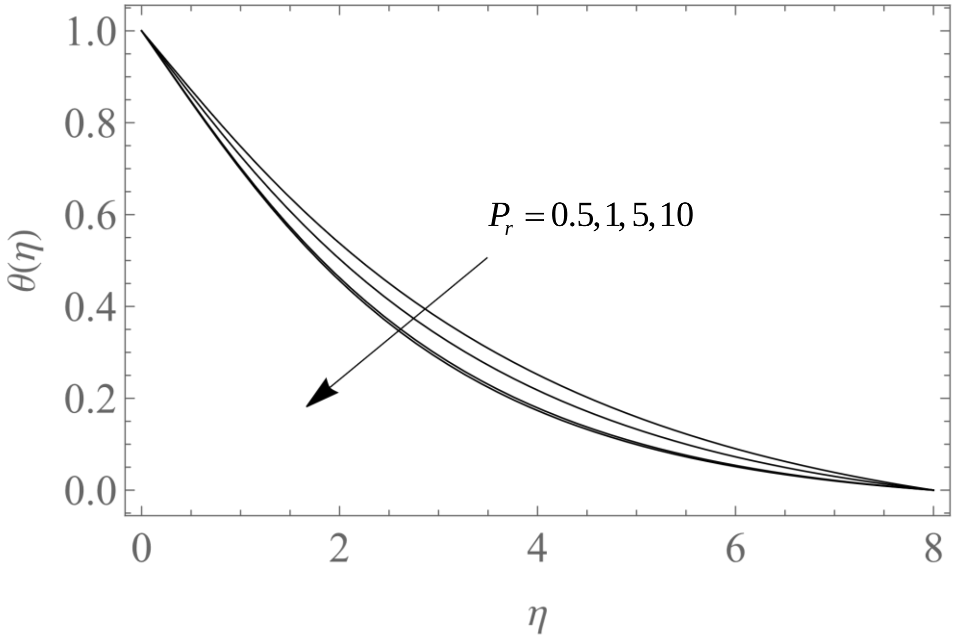

Fig 7: Impact of P_r on $\theta(\eta)$ with

$Le = 1, M = 1, E_c = 0.01, s = 0.01, K_c = 0.5, \inf = 8, R = 0.5, N_b = 0.1, N_t = 0.1,$

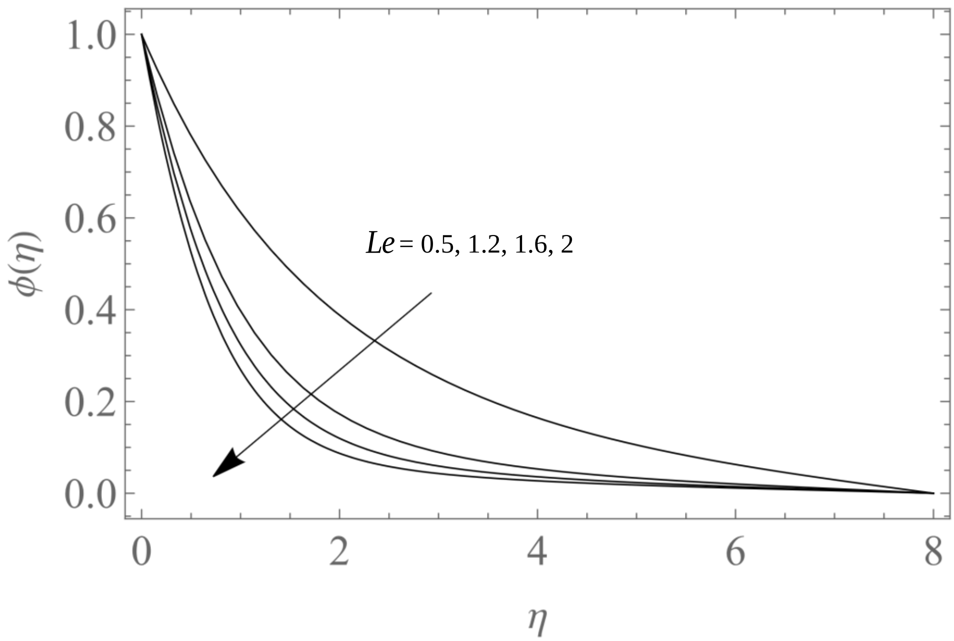

Fig 8: Impact of Le on $\phi(\eta)$ with

$P_r = 1, E_c = 0.01, s = 0.01, K_c = 0.5, M = 1, \inf = 8, R = 0.5, N_b = 0.1, N_t = 0.1$

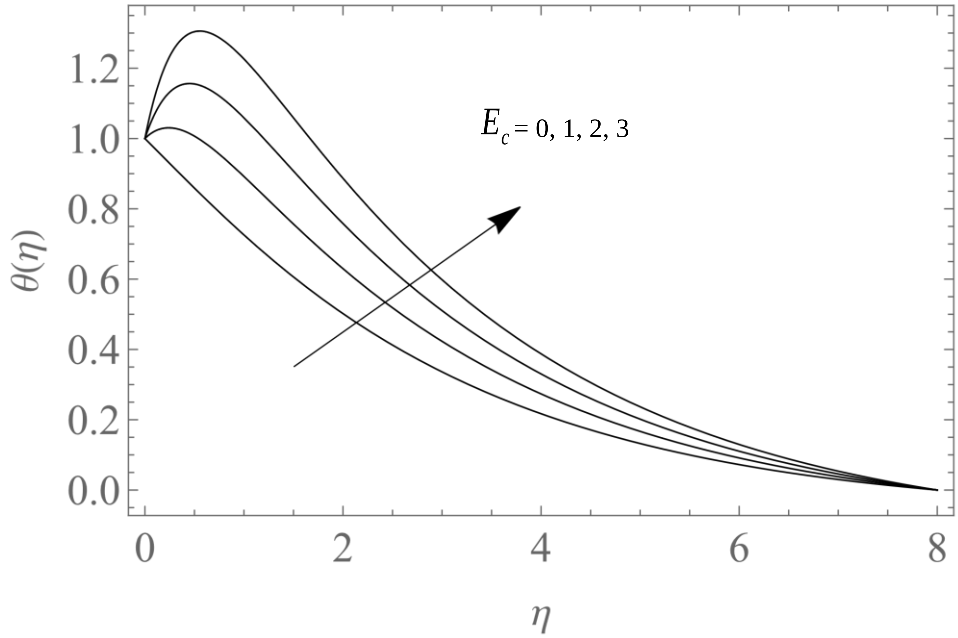

Fig 9: Impact of E_c on $\theta(\eta)$ with

$M=1, P_r=1, Le=1, K_c=0.5, \inf=8, s=0.01, R=0.5, N_b=0.1, N_t=0.1$

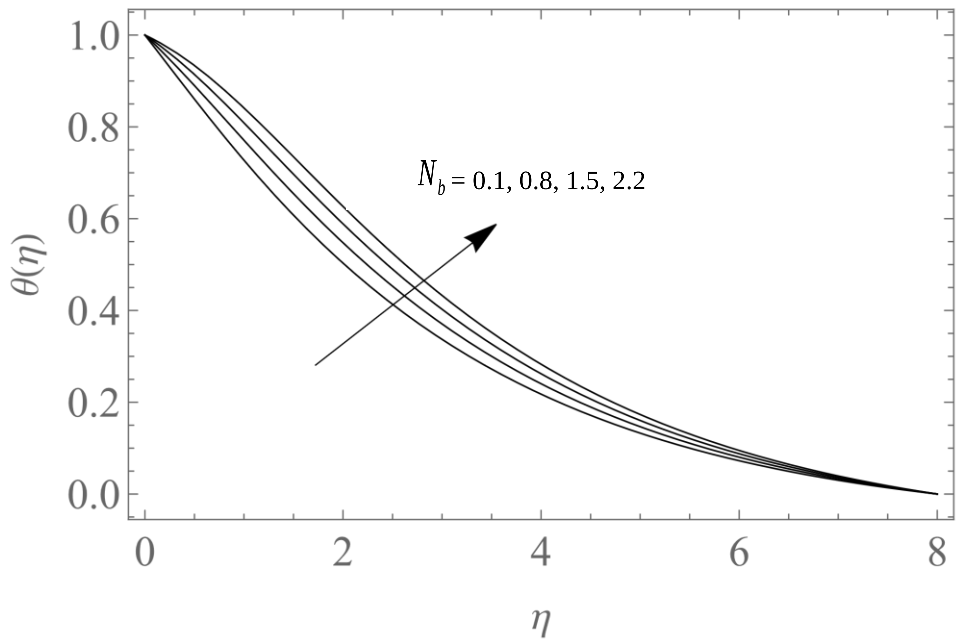

Fig 10: Impact of N_b on $\theta(\eta)$ with

$Le=1, P_r=1, , M=1, E_c=0.01, K_c=0.5, s=0.01, \inf=8, R=0.5, N_t=0.1$

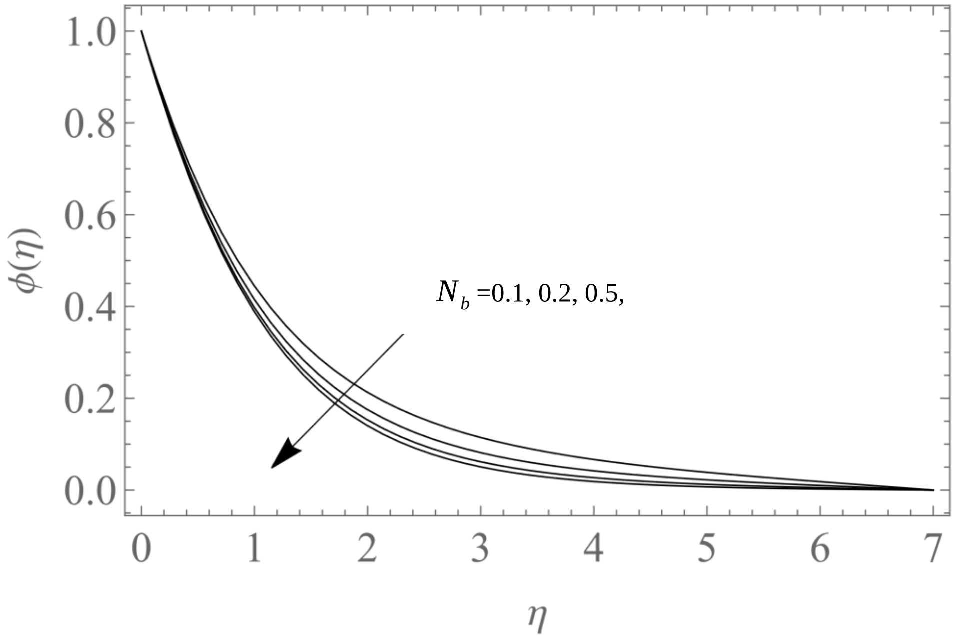

Fig 11: Impact of N_b on $\phi(\eta)$ with

$Le=1, P_r=1, M=1, E_c=0.01, K_c=0.5, s=0.01, \inf=8, R=0.5, N_t=0.1$

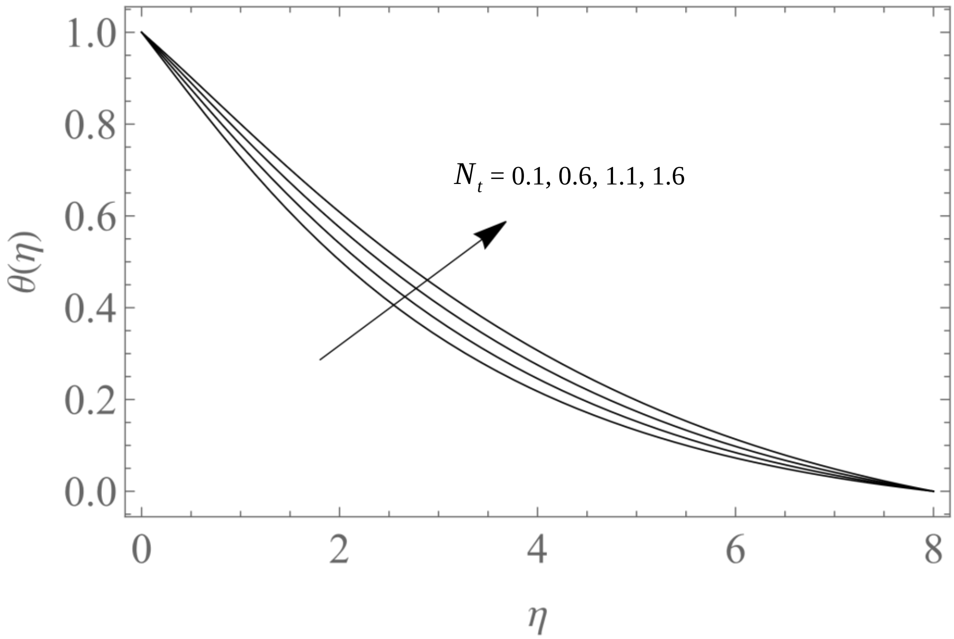

Fig 12: Impact of N_t on $\theta(\eta)$ with

$Le=1, P_r=1, M=1, E_c=0.01, K_c=0.5, s=0.01, \inf=8, R=0.5, N_b=0.1$

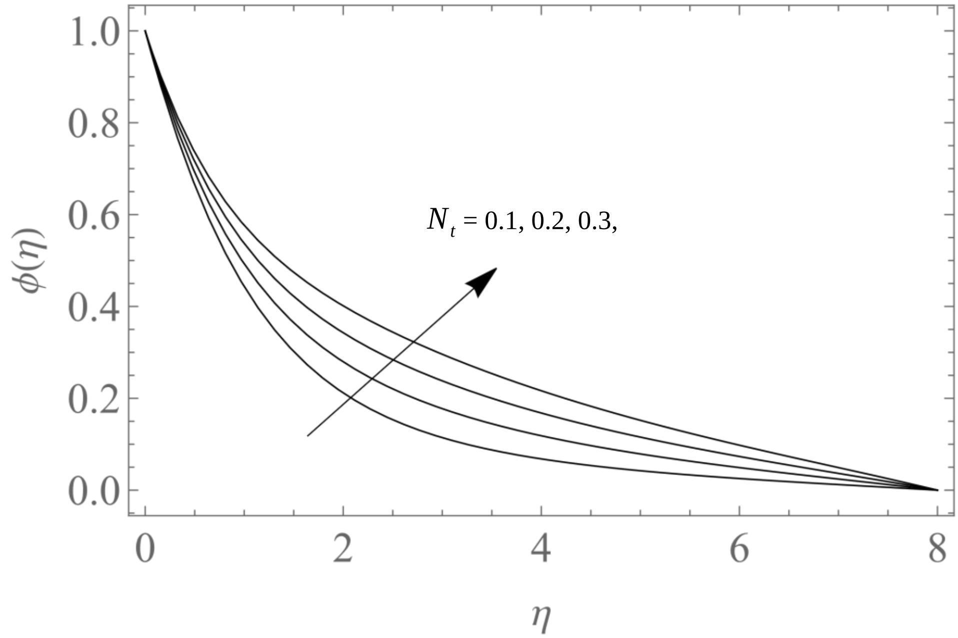

Fig 13: Impact of N_t on $\phi(\eta)$ with

$Le=1, P_r=1, M=1, E_c=0.01, K_c=0.5, \inf=8, s=0.01, R=0.5, N_b=0.1$

5. Conclusions

A numerical investigation is carried out on magneto hydrodynamic nanofluids through a stretching surface under the impact of chemical and radiation parameters. The following conclusions are derived.

1) The temperature profile rises when the radiation parameter (R) is increased.
2) The concentration appears to decrease as K_c is increased. The chemical reaction reduces the thickness of the boundary layer as a result.
3) Incremental change in $\Pr$ boost $\theta(\eta)$.
4) The thermal boundary layer thickness grows when the viscous dissipation parameter E_c rises. As a result, the temperature profile is increased.
5) As the Brownian motion parameter N_b is increased, the temperature profile rises, and the concentration profile falls.
6) The thickness of the temperature and nanoparticle concentration grows with the increase of N_t.
7) Nusselt number Nu_r decreases whereas Sherwood number Sh_r rises for the boosting values of R and K_c.

References

[1] S. Mansur, A. Ishak, I. Pop, Flow and heat transfer of nanofluid past stretching/shrinking sheet with partial slip boundary conditions, *Applied Mathematics and Mechanics,* Vol. 35, No. 11, pp. 1401-1410, 2014.

[2] M. Hamad, Analytical solution of natural convection flow of a nanofluid over a linearly stretching sheet in the presence of magnetic field, *International communications in heat and mass transfer,* Vol. 38, No. 4, pp. 487-492, 2011.

[3] K. Govardhan, G. Narender, G. S. Sarma, Heat and Mass transfer in MHD Nanofluid over a Stretching Surface along with Viscous Dissipation Effect, *International Journal of Mathematical, Engineering and Management Sciences*, Vol. 5, No. 2, pp. 343, 2020.
[4] G. Narender, S. Misra, K. Govardhan, Numerical Solution of MHD Nanofluid over a Stretching Surface with Chemical Reaction and Viscous Dissipation, *Chemical Engineering Research Bulletin*, Vol. 21, No. 1, pp. 36-45, 2019.
[5] P. Sreedevi, P. Sudarsana Reddy, A. Chamkha, Heat and mass transfer analysis of unsteady hybrid nanofluid flow over a stretching sheet with thermal radiation, *SN Applied Sciences*, Vol. 2, No. 7, pp. 1-15, 2020.
[6] M. Seddeek, M. Abdelmeguid, Effects of radiation and thermal diffusivity on heat transfer over a stretching surface with variable heat flux, *Physics Letters A*, Vol. 348, No. 3-6, pp. 172-179, 2006.
[7] A. Shafiq, G. Rasool, C. M. Khalique, S. Aslam, Second grade bioconvective nanofluid flow with buoyancy effect and chemical reaction, *Symmetry*, Vol. 12, No. 4, pp. 621, 2020.
[8] G. Narender, K. Govardhan, G. S. Sarma, Numerical study of radiative magnetohydrodynamics viscous nanofluid due to convective stretching sheet with the chemical reaction effect, *Iraqi Journal of Science*, pp. 1733-1744, 2020.
[9] P. Devaki, B. Venkateswarlu, S. Srinivas, S. Sreenadh, Mhd peristaltic flow of a nanofluid in a constricted artery for different shapes of nanosized particles, *Nonlinear Engineering*, Vol. 9, No. 1, pp. 51-59, 2020.
[10] M. Mohammadi, A. Farajpour, A. Moradi, M. Hosseini, Vibration analysis of the rotating multilayer piezoelectric Timoshenko nanobeam, *Engineering Analysis with Boundary Elements*, Vol. 145, pp. 117-131, 2022.
[11] M. Mohammadi, A. Rastgoo, Primary and secondary resonance analysis of FG/lipid nanoplate with considering porosity distribution based on a nonlinear elastic medium, *Mechanics of Advanced Materials and Structures*, Vol. 27, No. 20, pp. 1709-1730, 2020.
[12] M. Mohammadi, M. Hosseini, M. Shishesaz, A. Hadi, A. Rastgoo, Primary and secondary resonance analysis of porous functionally graded nanobeam resting on a nonlinear foundation subjected to mechanical and electrical loads, *European Journal of Mechanics-A/Solids*, Vol. 77, pp. 103793, 2019.
[13] M. Mohammadi, A. Rastgoo, Nonlinear vibration analysis of the viscoelastic composite nanoplate with three directionally imperfect porous FG core, *Structural Engineering and Mechanics, An Int'l Journal*, Vol. 69, No. 2, pp. 131-143, 2019.
[14] A. Farajpour, A. Rastgoo, M. Mohammadi, Vibration, buckling and smart control of microtubules using piezoelectric nanoshells under electric voltage in thermal environment, *Physica B: Condensed Matter*, Vol. 509, pp. 100-114, 2017.
[15] A. Farajpour, M. H. Yazdi, A. Rastgoo, M. Loghmani, M. Mohammadi, Nonlocal nonlinear plate model for large amplitude vibration of magneto-electro-elastic nanoplates, *Composite Structures*, Vol. 140, pp. 323-336, 2016.
[16] A. Farajpour, M. Yazdi, A. Rastgoo, M. Mohammadi, A higher-order nonlocal strain gradient plate model for buckling of orthotropic nanoplates in thermal environment, *Acta Mechanica*, Vol. 227, No. 7, pp. 1849-1867, 2016.
[17] M. Mohammadi, M. Safarabadi, A. Rastgoo, A. Farajpour, Hygro-mechanical vibration analysis of a rotating viscoelastic nanobeam embedded in a visco-Pasternak elastic medium and in a nonlinear thermal environment, *Acta Mechanica*, Vol. 227, No. 8, pp. 2207-2232, 2016.
[18] M. R. Farajpour, A. Rastgoo, A. Farajpour, M. Mohammadi, Vibration of piezoelectric nanofilm-based electromechanical sensors via higher-order non-local strain gradient theory, *Micro & Nano Letters*, Vol. 11, No. 6, pp. 302-307, 2016.
[19] M. Baghani, M. Mohammadi, A. Farajpour, Dynamic and stability analysis of the rotating nanobeam in a nonuniform magnetic field considering the surface energy, *International Journal of Applied Mechanics*, Vol. 8, No. 04, pp. 1650048, 2016.
[20] M. Goodarzi, M. Mohammadi, M. Khooran, F. Saadi, Thermo-mechanical vibration analysis of FG circular and annular nanoplate based on the visco-pasternak foundation, *Journal of Solid Mechanics*, Vol. 8, No. 4, pp. 788-805, 2016.
[21] H. Asemi, S. Asemi, A. Farajpour, M. Mohammadi, Nanoscale mass detection based on vibrating piezoelectric ultrathin films under thermo-electro-mechanical loads, *Physica E: Low-dimensional Systems and Nanostructures*, Vol. 68, pp. 112-122, 2015.
[22] M. Safarabadi, M. Mohammadi, A. Farajpour, M. Goodarzi, Effect of surface energy on the vibration analysis of rotating nanobeam, 2015.

[23] M. Goodarzi, M. Mohammadi, A. Gharib, Techno-Economic Analysis of Solar Energy for Cathodic Protection of Oil and Gas Buried Pipelines in Southwestern of Iran, in *Proceeding of*, https://publications.waset.org/abstracts/33008/techno-economic-analysis-of …, pp.

[24] M. Mohammadi, A. A. Nekounam, M. Amiri, The vibration analysis of the composite natural gas pipelines in the nonlinear thermal and humidity environment, in *Proceeding of*, https://civilica.com/doc/540946/, pp.

[25] M. Goodarzi, M. Mohammadi, M. Rezaee, Technical Feasibility Analysis of PV Water Pumping System in Khuzestan Province-Iran, in *Proceeding of*, https://publications.waset.org/abstracts/18930/technical-feasibility …, pp.

[26] M. Mohammadi, A. Farajpour, A. Moradi, M. Ghayour, Shear buckling of orthotropic rectangular graphene sheet embedded in an elastic medium in thermal environment, *Composites Part B: Engineering,* Vol. 56, pp. 629-637, 2014.

[27] M. Mohammadi, A. Moradi, M. Ghayour, A. Farajpour, Exact solution for thermo-mechanical vibration of orthotropic mono-layer graphene sheet embedded in an elastic medium, *Latin American Journal of Solids and Structures,* Vol. 11, pp. 437-458, 2014.

[28] M. Mohammadi, A. Farajpour, M. Goodarzi, F. Dinari, Thermo-mechanical vibration analysis of annular and circular graphene sheet embedded in an elastic medium, *Latin American Journal of Solids and Structures*, Vol. 11, pp. 659-682, 2014.

[29] M. Mohammadi, A. Farajpour, M. Goodarzi, Numerical study of the effect of shear in-plane load on the vibration analysis of graphene sheet embedded in an elastic medium, *Computational Materials Science,* Vol. 82, pp. 510-520, 2014.

[30] A. Farajpour, A. Rastgoo, M. Mohammadi, Surface effects on the mechanical characteristics of microtubule networks in living cells, *Mechanics Research Communications,* Vol. 57, pp. 18-26, 2014.

[31] S. R. Asemi, M. Mohammadi, A. Farajpour, A study on the nonlinear stability of orthotropic single-layered graphene sheet based on nonlocal elasticity theory, *Latin American Journal of Solids and Structures,* Vol. 11, pp. 1541-1546, 2014.

[32] M. Goodarzi, M. Mohammadi, A. Farajpour, M. Khooran, Investigation of the effect of pre-stressed on vibration frequency of rectangular nanoplate based on a visco-Pasternak foundation, 2014.

[33] S. Asemi, A. Farajpour, H. Asemi, M. Mohammadi, Influence of initial stress on the vibration of double-piezoelectric-nanoplate systems with various boundary conditions using DQM, *Physica E: Low-dimensional Systems and Nanostructures,* Vol. 63, pp. 169-179, 2014.

[34] S. Asemi, A. Farajpour, M. Mohammadi, Nonlinear vibration analysis of piezoelectric nanoelectromechanical resonators based on nonlocal elasticity theory, *Composite Structures,* Vol. 116, pp. 703-712, 2014.

[35] M. Mohammadi, M. Ghayour, A. Farajpour, Free transverse vibration analysis of circular and annular graphene sheets with various boundary conditions using the nonlocal continuum plate model, *Composites Part B: Engineering,* Vol. 45, No. 1, pp. 32-42, 2013.

[36] M. Mohammadi, M. Goodarzi, M. Ghayour, A. Farajpour, Influence of in-plane pre-load on the vibration frequency of circular graphene sheet via nonlocal continuum theory, *Composites Part B: Engineering,* Vol. 51, pp. 121-129, 2013.

[37] M. Mohammadi, A. Farajpour, M. Goodarzi, R. Heydarshenas, Levy type solution for nonlocal thermo-mechanical vibration of orthotropic mono-layer graphene sheet embedded in an elastic medium, *Journal of Solid Mechanics,* Vol. 5, No. 2, pp. 116-132, 2013.

[38] M. Mohammadi, A. Farajpour, M. Goodarzi, H. Mohammadi, Temperature Effect on Vibration Analysis of Annular Graphene Sheet Embedded on Visco-Pasternak Foundati, *Journal of Solid Mechanics,* Vol. 5, No. 3, pp. 305-323, 2013.

[39] M. Danesh, A. Farajpour, M. Mohammadi, Axial vibration analysis of a tapered nanorod based on nonlocal elasticity theory and differential quadrature method, *Mechanics Research Communications,* Vol. 39, No. 1, pp. 23-27, 2012.

[40] A. Farajpour, A. Shahidi, M. Mohammadi, M. Mahzoon, Buckling of orthotropic micro/nanoscale plates under linearly varying in-plane load via nonlocal continuum mechanics, *Composite Structures,* Vol. 94, No. 5, pp. 1605-1615, 2012.

[41] M. Mohammadi, M. Goodarzi, M. Ghayour, S. Alivand, Small scale effect on the vibration of orthotropic plates embedded in an elastic medium and under biaxial in-plane pre-load via nonlocal elasticity theory, 2012.

[42] A. Farajpour, M. Mohammadi, A. Shahidi, M. Mahzoon, Axisymmetric buckling of the circular graphene sheets with the nonlocal continuum plate model, *Physica E: Low-dimensional Systems and Nanostructures,* Vol. 43, No. 10, pp. 1820-1825, 2011.

[43] A. Farajpour, M. Danesh, M. Mohammadi, Buckling analysis of variable thickness nanoplates using nonlocal continuum mechanics, *Physica E: Low-dimensional Systems and Nanostructures,* Vol. 44, No. 3, pp. 719-727, 2011.

[44] H. Moosavi, M. Mohammadi, A. Farajpour, S. Shahidi, Vibration analysis of nanorings using nonlocal continuum mechanics and shear deformable ring theory, *Physica E: Low-dimensional Systems and Nanostructures,* Vol. 44, No. 1, pp. 135-140, 2011.

[45] M. Mohammadi, M. Ghayour, A. Farajpour, Analysis of free vibration sector plate based on elastic medium by using new version differential quadrature method, *Journal of solid mechanics in engineering,* Vol. 3, No. 2, pp. 47-56, 2011.

[46] A. Farajpour, M. Mohammadi, M. Ghayour, Shear buckling of rectangular nanoplates embedded in elastic medium based on nonlocal elasticity theory, in *Proceeding of,* www.civilica.com/Paper-ISME19-ISME19_390.html, pp. 390.

[47] M. Mohammadi, A. Farajpour, A. R. Shahidi, Higher order shear deformation theory for the buckling of orthotropic rectangular nanoplates using nonlocal elasticity, in *Proceeding of,* www.civilica.com/Paper-ISME19-ISME19_391.html, pp. 391.

[48] M. Mohammadi, A. Farajpour, A. R. Shahidi, Effects of boundary conditions on the buckling of single-layered graphene sheets based on nonlocal elasticity, in *Proceeding of,* www.civilica.com/Paper-ISME19-ISME19_382.html, pp. 382.

[49] M. Mohammadi, M. Ghayour, A. Farajpour, Using of new version integral differential method to analysis of free vibration orthotropic sector plate based on elastic medium, in *Proceeding of,* www.civilica.com/Paper-ISME19-ISME19_497.html, pp. 497.

[50] N. Ghayour, A. Sedaghat, M. Mohammadi, Wave propagation approach to fluid filled submerged visco-elastic finite cylindrical shells, 2011.

[51] M. Mohammadi, A. Farajpour, A. Rastgoo, Coriolis effects on the thermo-mechanical vibration analysis of the rotating multilayer piezoelectric nanobeam, *Acta Mechanica*, https://doi.org/10.1007/s00707-022-03430-0, 2023.

[52] N. Y. Abd Elazem, Numerical results for influence the flow of MHD nanofluids on heat and mass transfer past a stretched surface, *Nonlinear Engineering,* Vol. 10, No. 1, pp. 28-38, 2021.

[53] W. Khan, I. Pop, Boundary-layer flow of a nanofluid past a stretching sheet, *International journal of heat and mass transfer,* Vol. 53, No. 11-12, pp. 2477-2483, 2010.